Protein Kinase C θ Affects Ca^{2+} Mobilization and NFAT Cell Activation in Primary Mouse T Cells

Christa Pfeifhofer,[1] Kurt Kofler,[1] Thomas Gruber,[1]
Nassim Ghaffari Tabrizi,[1] Christina Lutz,[1] Karl Maly,[2] Michael Leitges,[3]
and Gottfried Baier[1]

[1]*Institute of Medical Biology and Human Genetics and* [2]*Institute of Medical Biochemistry, University of Innsbruck, A-6020 Innsbruck, Austria*

[3]*Max-Planck Institute for Experimental Endocrinology, D-30625 Hannover, Germany*

Abstract

Protein kinase C (PKC)θ is an established component of the immunological synapse and has been implicated in the control of AP-1 and NF-κB. To study the physiological function of PKCθ, we used gene targeting to generate a PKCθ null allele in mice. Consistently, interleukin 2 production and T cell proliferative responses were strongly reduced in PKCθ-deficient T cells. Surprisingly, however, we demonstrate that after CD3/CD28 engagement, deficiency of PKCθ primarily abrogates NFAT transactivation. In contrast, NF-κB activation was only partially reduced. This NFAT transactivation defect appears to be secondary to reduced inositol 1,4,5-trisphosphate generation and intracellular Ca^{2+} mobilization. Our finding suggests that PKCθ plays a critical and nonredundant role in T cell receptor–induced NFAT activation.

Key words: T lymphocyte • PKCθ • TCR/CD3 • Ca^{2+} response • NFAT

Introduction

The protein kinase C (PKC)* is not a single entity but constitutes, at the gene level, nine different isotypes: PKCα, β, γ, δ, ε, ζ, η, θ, and ι. However, their nonredundant functions remain mostly unresolved (for review see 1). Among the PKC family, PKCθ is predominantly expressed in T lymphocytes (2–4) and it has been shown that overexpression or inhibition of PKCθ in T cell lines can affect activation of the IL-2 promoter (5–7). In T cell lines, PKCθ thereby mediates activation of activator protein 1 (AP-1; references 5–8) and nuclear factor (NF)-κB (9–13). The physiological role of PKCθ in TCR/CD28-induced AP-1 and NF-κB activation was established in the first mouse genetic analysis of PKCθ (14).

PKCθ selectively localizes into the center of the mature i-synapse during antigen stimulation (15). TCR/CD3 stimulation was essential for recruitment and enzymatic activation of PKCθ (10, 13, 16) and this was found to be mediated by a nonconventional PI-3K/Vav-1–dependent pathway (17–19) and not dependent on phospholipase C-γ1 (PLCγ1) and diacylglycerol formation (known to otherwise nonspecifically activate all T cell–expressed conventional and novel isotypes, PKCα, β, and δ, ε, η, and θ, respectively; reference 20).

To further investigate the critical role of PKCθ, we independently generated PKCθ-deficient mice. Analysis of our PKCθ-deficient T cells revealed reduced proliferation and IL-2 production, entirely consistent with the previous work (5, 8–14). The observed role of PKCθ in TCR/CD28-induced AP-1 and NF-κB activation was already evident from the first mouse genetic analysis of PKCθ (14). However, unexpectedly and in contrast to Sun et al. (14), here we report that PKCθ is involved in TCR-induced Ca^{2+} responses and that TCR-mediated NFATp and NFATc transactivation is primarily impaired in PKCθ-deficient mature $CD3^+$ T cells. These findings provide genetic evidence that PKCθ may exert an unexpected proximal role upstream of PLCγ1.

Materials and Methods

Generation of PKC$\theta^{\Delta/\Delta}$ Mice. A genomic PKCθ clone, containing the exons 2–4 encoding the AUG start codon (for the gene locus organization, see 21), was isolated from a 129/J library and used to construct the targeting vector (see Fig. 1 A). E14 ES

C. Pfeifhofer and K. Kofler contributed equally to this work.

Address correspondence to Gottfried Baier, Institute of Medical Biology and Human Genetics, University of Innsbruck, Schoepfstraße 41, A-6020 Innsbruck, Austria. Phone: 43-512-507-3451; Fax: 43-512-507-2861; E-mail: Gottfried.Baier@uibk.ac.at

**Abbreviations used in this paper:* AP-1, activator protein 1; CCE, capacitative Ca^{2+} entry; EMSA, electrophoretic mobility shift assay; IP_3, inositol 1,4,5-trisphosphate; NF, nuclear factor; PDBu, phorbol ester; PKC, protein kinase C; PLCγ1, phospholipase C-γ1.

cells were transfected with linearized targeting vector and after the selection of colonies with G418, homologous recombination events were identified by Southern blot analysis and obtained at a frequency of 1:100. The PKCθflox allele we generated is a extended allele, owing to the presence of a floxed (flanked by loxP sequences) neo expression cassette inserted in the unique SpeI site within intron 2 (see Fig. 1 A). A third loxP site was inserted into the PstI site in intron 4. Positive clones were used to generate chimaeric founder mice by microinjection into C57BL/6J blastocysts, generating a conditional PKCθ knockout mouse. Germline transmission was confirmed by Southern blot analysis of tail DNA. PKCθflox/+ females were crossed with C57BL/6J males ubiquitously expressing the Cre transgene ($Cre^{+/-}$), resulting in complete gene deletion of the PKCθflox allele in $PKC\theta^{flox/+}$ $Cre^{+/-}$ mice. DNA was extracted from adult tail tissue, digested with BglII, and hybridized with an endogenous 3′-probe (indicated in Fig. 1 A) distinguishing wild-type (+/+), heterozygote mutant (+/Δ), and homozygote mutant (Δ/Δ) alleles (see Fig. 1 B). Alternatively, mice carrying $PKC\theta^{\Delta/\Delta}$ were routinely genotyped by PCR (see Fig. 1 C) using the primers E5.2-S (5′-GCA GAC CCA GAC CAT TCC CTA G-3′)/E10.5–3 (5′-GGT AGT CTC GGA TGG TTG AGG G-3′) to detect the mutant allele (2kb product) and E5.2-S (same as above)/E5.2-CRE (5′-CGC ATT CGT CTA CAT GAT AAC CGA C-3′) to detect the wild-type allele (1.2-kb product). Homozygote PKCθ mutant (Δ/Δ) mice were further backcrossed into C57BL/6J background ($n = 3$) before functional analysis.

Apoptosis in Thymocytes and Mature Lymphocytes. Freshly isolated thymocytes from 6–8-wk-old mice were plated at 5×10^6 cells ml^{-1}. Cells were stimulated for 24 h with 10 μg ml^{-1} anti-CD3 and camptothecin (0.5 and 1 μM), stained with propidium iodide (0.005% propidium iodide, 0.1% Na citrate, and 0.1% Triton X-100), and viability was determined by flow cytometry.

Flow Cytometry. Single cell suspensions were prepared and incubated for 30 min on ice in staining buffer (phosphate-buffered saline containing 2% FCS and 0.2% NaN_3) with fluorescein isothiocyanate and phycoerythrin antibodies. Surface marker expression of thymocytes, splenocytes, or lymph nodes was analyzed using a FACScan™ cytometer (Becton Dickinson) and CellQuest™ software according to standard protocols. Antibodies against murine CD3 (145-2C11), CD4, and CD8 were obtained from Caltag Laboratories and CD28(37.51), CD69, CD44, and CD25 and were obtained from BD Biosciences.

Proliferation Assays. Mature $CD3^+$ T cells were purified from pooled spleen and lymph nodes with mouse T cell enrichment columns (R&D Systems). T cell populations were typically 95% $CD3^+$ as determined by staining and flow cytometry. Thymocytes were prepared directly from freshly isolated thymi. For anti-CD3 stimulations, 5×10^5 T cells in 200 μl proliferation medium (RPMI supplemented with 10% FCS, 2 mM L-glutamine, and 50 units ml^{-1} penicillin/streptomycin) were added in duplicates to 96-well plates precoated with 10 μg ml^{-1} anti-CD3 antibody (clone 2C11). Alternatively, 10 ng ml^{-1} phorbol ester (PDBu; Sigma-Aldrich) plus Ca^{2+} ionophore (ionomycin, 50–500 ng ml^{-1} as indicated; Sigma-Aldrich) were used. Where indicated, IL-2 (final concentration 40 units ml^{-1}) or soluble 1 μg ml^{-1} anti-CD28 was also added. Cells were harvested at 64 h after a 16-h pulse with 1 μCi [^{3}H]thymidine per well and incorporation of [^{3}H]thymidine was measured with a Matrix 96 direct β counter system. For the mixed lymphocyte reaction assays, T cells were purified from littermate mice (B6 background) and mixed in duplicates at various densities with mitomycin C–treated splenocytes from BALB/c mice. After 48 h of growth, the cells were pulsed for 16 h with 1 μCi [^{3}H]thymidine.

IL-2 Production. IL-2 produced from the cultures was measured via the IL-2–dependent indicator cell line CTLL-2. T cells were plated in 96-well plates and incubated with the described stimuli. Plates were then frozen at −20°C. After centrifugation, supernatants were added to CTLL-2 cells (10^4/well) and cultured for an additional 48 h and pulsed for 6 h with 1 μCi [^{3}H]thymidine per well. A standard curve was established by using recombinant IL-2.

Western Blot Analysis. T cells were stimulated with PBS (control), solid phase hamster anti–CD3 (clone 145-2C11; BD Biosciences), or solid phase hamster anti–CD3 (clone 145-2C11) plus hamster anti–CD28 (clone 37.51; BD Biosciences) at 37°C for various time periods. Cells were lysed in ice cold lysis buffer (5 mM NaP_2P, 5 mM NaF, 5 mM EDTA, 50 mM NaCl, 50 mM Tris, pH 7.3, 2% NP-40, 50 μg/ml each aprotinin, and leupeptin) and centrifuged at 15,000 *g* for 15 min at 4°C. Protein lysates or immunoprecipitates were subjected to Western blotting using antibodies against PKCθ, δ, ε, and ζ/ι (Santa Cruz Biotechnology, Inc.) or PKCα and Fyn (Upstate Biotechnology). Cell fractionation was performed by lysis in equivalent amounts of different buffers (s fraction: soluble, without detergent; pt fraction: particulate, containing 1% NP-40; ns fraction: nonsoluble, containing 2% SDS). To detect the transcription factors, mAb 7A6 for NFATc (Affinity BioReagents, Inc.), mAbG1-D10 for NFATp (Santa Cruz Biotechnology, Inc.), and pAb for cfos, cJun, and p50 (Geneka) were used. Tyrosine phosphorylation was monitored in total cell lysates and PLCγ1 immunoprecipitates using an antiphosphotyrosine mAb (4G10; Upstate Biotechnology) and a pAb reactive to $(p)Y^{783}$ of PLCγ1 (Biosource International).

Gel Mobility Shift Assays. Nuclear extracts were harvested from 2×10^7 cells according to standard protocols. Mature $CD3^+$ T cells were purified from pooled spleen and lymph nodes, washed in PBS, and resuspended in 10 mM Hepes, pH 7.9, 10 mM KCl, 0.1 mM EDTA, 0.1 mM EGTA, 1 mM DTT, and protease inhibitors. Cells were incubated on ice for 15 min. NP-40 was added to a final concentration of 0.6%, the cells were vigorously vortex mixed, and the mixture was centrifuged for 5 min. The nuclear pellets were washed twice and resuspended in 20 mM Hepes, pH 7.9, 0.4 M NaCl, 1 mM EDTA, 1 mM EGTA, 1 mM DTT, and protease inhibitors, and the tube was rocked for 30 min at 4°C. After centrifugation for 10 min, the supernatant was collected. 2 μg extract proteins were incubated in binding buffer with end-labeled, double stranded oligonucleotide probes (NF-κB: 5′-GCC ATG GGG GGA TCC CCG AAG TCC-3′; AP-1: 5′-CGC TTG ATG ACT CAG CCG GAA-3′; and NFAT: 5′-GCC CAA AGA GGA AAA TTT GTT TCA TAC AG-3′). 3×10^5 cpm of labeled probe was used in each reaction and band shifts were resolved on 5% polyacrylamide gels. All experiments have been performed at least three times with similar outcomes.

Intracellular Calcium Measurements. For dye loading, 5×10^6 freshly isolated mature $CD3^+$ T cells, from pooled spleen and lymph nodes, were loaded for 30 min with fura-2 acetoxymethylester (Molecular Probes). For detection of cytosolic Ca^{2+}, cells were incubated with 5 μg ml^{-1} biotinylated anti-CD3 (clone 145-2C11; BD Biosciences) for 15 min at 4°C. Cells were washed with Hepes buffer (HBS: 20 mM Hepes/NaOH, pH 7.4, 140 mM NaCl, 5 mM KCl, 1 mM $CaCl_2$, 0.5 mM $MgCl_2$, 5.5 mM glucose) and anti-CD3 molecules were cross-linked at room temperature using 5 μg ml^{-1} streptavidin (Sigma-Aldrich). For determination of the cytoplasmic Ca^{2+} concentration ($[Ca^{2+}]_i$), fluorescence was measured by a Spex Fluorolog 2 spectrofluorometer (CM-1)

equipped with two excitation monochrometers and a chopper system as previously described (22). Nanomolar values of cytoplasmic Ca^{2+} concentration were calculated from the ratios of background subtracted images (excitation wavelength 350 and 385 nm, emission wavelength 510 nm) according to the calibration procedure and equations previously described (23). Experiments have been performed at least four times with similar outcomes.

Inositol 1,4,5-Trisphosphate (IP_3) Measurement. Mature $CD3^+$ T cells were stimulated by cross-linking of CD3 as described above. The stimulations were terminated by the addition of ice cold TCA followed by 15 min of incubation on ice. The samples were centrifuged at 1,400 *g* at 4°C for 15 min, and the supernatant was extracted with 10 vol water-saturated diethyl ether neutralized with 1 M $NaHCO_3$. IP_3 was quantitated in duplicate samples using a competitive $[^3H]IP_3$ binding assay (Amersham Biosciences) according to the manufacturer's instructions. Experiments have been performed at least three times in duplicates with similar outcomes.

Results

Generation of PKC$\theta^{\Delta/\Delta}$ Mice. To study the in vivo function of PKCθ in mice, we generated a null allele (from the conditional allele, PKCθflox) using the Cre/loxP system. The PKCθ mutation (deletion of exons 3 and 4 encoding amino acids 10–87) resulted in a frame shift after amino acid residue 9 of mouse PKCθ (Fig. 1 A). However, the selectively testis-expressed PKCθII mRNA variant (via alternative splicing from a PKCθII-specific exon located between exons 7 and 8 of the PKCθI wild-type gene; reference 24) has not been disrupted by our targeting strategy. ES cell lines heterozygous for the mutation at the PKCθ locus were used to generate chimeric mice, which were backcrossed to C57BL/6J to obtain heterozygous PKCθ mice. The intercross of these mice produced homozygous PKCθ-deficient (Δ/Δ) mutant mice, which are distinguishable by Southern blot and/or PCR genotyping (Fig. 1, B and C). The null mutation of PKCθ in thymocytes as well as mature T lymphocytes derived from PKC$\theta^{\Delta/\Delta}$ mice was confirmed by Western blotting using two distinct epitopes within the PKCθ protein. Consistent with our targeting strategy, no PKCθ protein could be detected. This includes no aberrant T cell expression of PKCθII (Fig. 1, D and E).

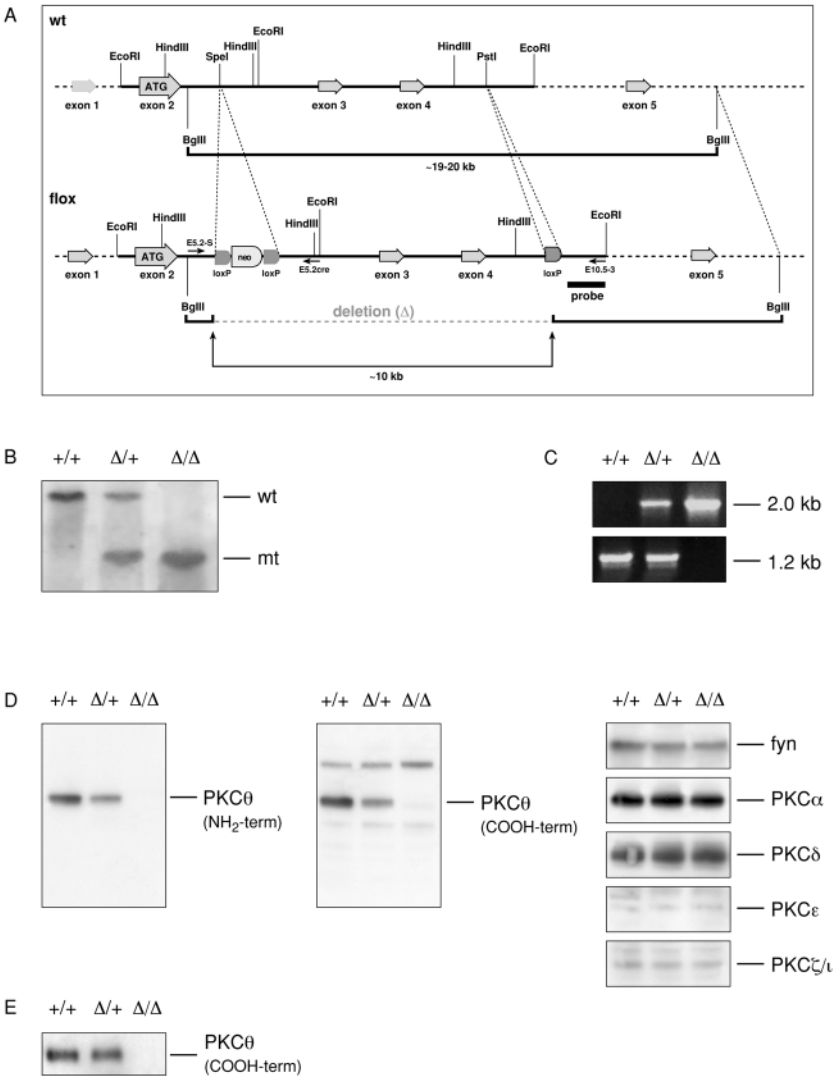

Figure 1. Targeted disruption of the PKCθ locus. (A) Schematic representation of the murine wild-type PKCθ locus (top) showing NH_2-terminal exons (1–5, open arrows) and the PKCθ conditional knockout allele (flox). Due to targeting vector design, Cre-mediated recombination deletes the complete coding sequence of exons 3 and 4, inducing a frame shift mutation between exons 2 and 5, resulting in an only 9 amino acid residual open reading frame of the mutated PKCθ^{Δ} locus. The position of the 3′ flanking probe as well as PCR primers E5.2-Cre, E5.2-S, and E10.5-3, which were used for genotyping, are indicated. (B) Genomic DNA was digested with BglII and hybridized to the 3′ flanking probe. Wild-type and mutant$^{\Delta}$ bands are indicated. (C) PCR genotyping using primer pairs E5.2-S/E10.5-3 (to detect a 2 kb mutant$^{\Delta}$ allele-derived product) and E5.2-S/E5.2-CRE (to detect a 1.2-kb wild-type^{+} allele-derived product). (D and E) Western blot analysis of 5×10^6/lane thymocytes (D) and mature purified $CD3^+$ T cells (E). Antibodies were directed against PKCθ (using distinct epitopes in N or C terminus, respectively), PKCα, δ, ε, ζ/ι, and $p59^{fyn}$, with the latter as loading control, as indicated.

As controls, neither thymocyte-expressed PKC isotypes tested, e.g. PKCα, δ, ε, nor ζ/ι showed any deregulated expression levels in T cells derived from PKCθ$^{\Delta/\Delta}$ mice.

PKCθ$^{\Delta/\Delta}$ mice were born at the expected Mendelian frequency, were fertile, and appeared healthy and anatomically normal as tested up to 9 mo of age. Thymocyte numbers and development appeared to be unaffected by the PKCθ mutation. Double-positive thymocytes were able to differentiate into normal total numbers of CD4$^+$ or CD8$^+$ T cells, which expressed normal levels of CD3 (Table I). Moreover, the relative and total numbers of mature CD4$^+$ and CD8$^+$ T cells in the lymph nodes and spleen were comparable between PKCθ$^{\Delta/\Delta}$ and wild-type littermates. In addition, no significant difference in the susceptibility of thymocytes as well as mature T lymphocytes from adult PKCθ$^{\Delta/\Delta}$ mice to ex vivo apoptotic stimuli was observed (not depicted).

Impaired Antigen Receptor–induced Proliferation and Activation of PKCθ-deficient T Lymphocytes. Because of PKCθ's predominant expression in lymphocytes of the T cell lineage (2–4), we then investigated TCR/CD3 signaling functions in T cells. Activation of resting T lymphocytes (resulting in IL-2 cytokine secretion and subsequent proliferation) is known to require stimulation of the TCR–CD3 complex (plus the CD28 auxiliary receptor) or treatment with pleiotropic PDBu plus Ca^{2+} ionophore. As a result, purified mature T cells (Fig. 2 A) from wild-type mice proliferated upon stimulation with plate-bound agonistic anti-CD3 antibody (with or without anti-CD28 costimulation). However, PKCθ$^{\Delta/\Delta}$ T cells neither proliferated well in response to anti-CD3 nor anti-CD3/anti-CD28 stimuli. Similarly, PKCθ$^{\Delta/\Delta}$ thymocytes demonstrated reduced proliferation rates when compared with wild-type thymocytes (not depicted). The addition of exogenous IL-2 at 40 units ml^{-1} almost completely restored the anti-CD3–induced proliferative response of the mutant T cells, indicating that the CD25 surface expression (see below) as well as signaling events downstream of this IL-2 high affinity cytokine receptor remained mostly intact. Treatment with PDBu in combination with Ca^{2+} ionophore (ionomycin) induced comparable proliferation of wild-type as well as PKCθ$^{\Delta/\Delta}$ T cells (Fig. 2 B). This finding suggests that the signaling elements downstream of the antigen receptor remain mostly intact. In addition, it indicates that recruitment of other T cell–expressed conventional or novel PKC isotypes as well as RasGRP (responsive to PDBu/diacylglycerol) may compensate for the absence of PKCθ to restore the biological response.

The marked decrease in proliferation, observed in PKCθ-deficient mature T cells stimulated with anti-CD3 (with or without anti-CD28 costimulation) was accompanied by a significant albeit not complete reduction in the level of secreted IL-2 (Fig. 3 A). Similarly, PKCθ-deficient thymocytes demonstrated significant reduction in the level of secreted IL-2 (not depicted). In response to either of these stimuli, neither proliferation (Fig. 2 A) nor IL-2 secretion (Fig. 3 A) of mature T cells from the heterozygous PKCθ$^{\Delta/+}$ mice was reduced relative to that of wild-type T cells indicating haplosufficiency. Again, treatment with PDBu plus ionomycin induced comparable IL-2 secretion of wild-type as well as PKCθ$^{\Delta/\Delta}$ T cells. Thus, loss of PKCθ in T cells results in partially defective IL-2 cytokine production and cell cycle progression. However, in the absence of PKCθ, T cell proliferation and IL-2 secretion defects were restored by treatment with PDBu plus Ca^{2+}

Table I. *Flow Cytometric Analyses of PKCθ$^{\Delta/\Delta}$ Thymocytes*

Cell subset	Wild-type	PKCθ$^{\Delta/\Delta}$
Thymus		
CD4$^+$ CD8$^+$	91.5 ± 0.28	91.02 ± 0.33
CD4$^+$ CD8$^-$	5.94 ± 0.29	6.88 ± 0.34
CD4$^-$ CD8$^+$	1.03 ± 0.13	0.84 ± 0.04
CD4$^-$ CD8$^-$	1.54 ± 0.13	1.27 ± 0.02
CD3$^+$	21.73 ± 0.95	29.37 ± 0.31

Consistently, cellularity of spleens and lymph nodes was comparable in wild-type and PKCθ$^{\Delta/\Delta}$ mice (not depicted).
Percentages ± SEM of positive cells per total cells.

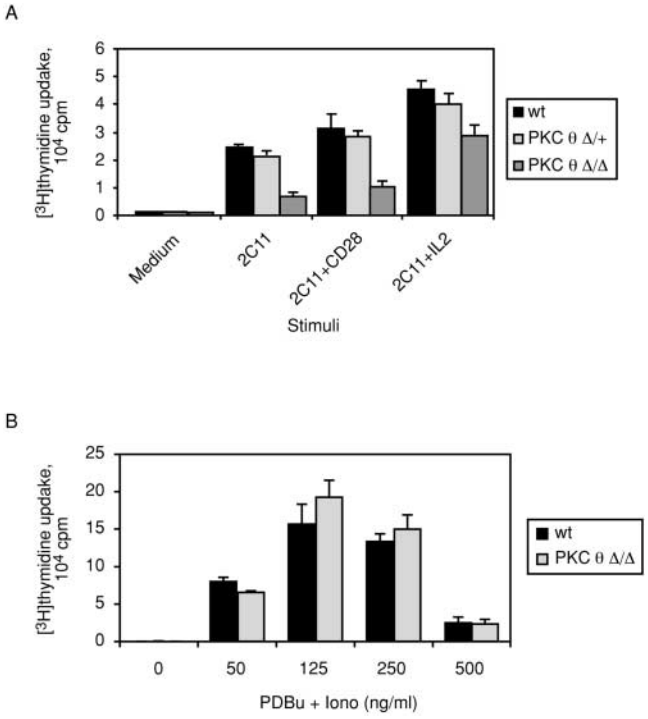

Figure 2. Impaired T cell activation in PKCθ$^{\Delta/\Delta}$ mice. Proliferative responses of purified mature CD3$^+$ T cells of wild-type (wt), PKCθ$^{\Delta/+}$, and PKCθ$^{\Delta/\Delta}$. After incubation with medium alone and (A) various stimuli such as anti-CD3 (96-well plates were precoated with a concentration of 10 μg ml^{-1}), with or without 1 μg ml^{-1} soluble anti-CD28, 40 units ml^{-1} human, recombinant IL-2, or (B) 10 ng ml^{-1} PDBu and ionomycin (at a range from 50 to 500 ng ml^{-1}, as indicated) for 48 h, cultures were pulsed for 16 h with 1 μCi [^{3}H]thymidine per well and cells were then harvested and analyzed using standard procedures. Results shown are the mean ± SD [^{3}H]thymidine incorporation of at least five independent experiments.

ionophore (Figs. 2 B and 3 A), stimuli known to bypass antigen receptor ligation. This indicates that the PKCθ-dependent and unique upstream pathway specific for TCR engagement is distinct from pathways used by pleiotropic PDBu-induced PKC activation.

Using the primary mixed lymphocyte reaction assay, we evaluated wild-type as well as PKCθ$^{\Delta/\Delta}$ mature T cell proliferation induced by allogenic MHC expressed on BALB/c mice–derived splenocytes. Consistent with the results presented in Fig. 2 A, a significant decrease in proliferation was observed in PKCθ-deficient T cells (Fig. 3 B). Cotreatment with exogenous IL-2 at 40 units ml^{-1} or treatment with PDBu/ionomycin restored almost normal proliferative responses of the PKCθ$^{\Delta/\Delta}$ T cells (not depicted). Consistent with the phenotype of our null allele PKCθ$^{\Delta/\Delta}$, PKCθ-deficient T cells from the first knockout mouse did produce less IL-2 and failed to proliferate strongly in response to TCR or allogenic MHC stimulation (14).

TCR-induced S phase entry of resting T cells is known to promote transcriptional up-regulation of IL-2 as well as IL-2 receptor α chain (CD25) genes, thereby constituting the autocrine cycle of IL-2 cytokine and its high affinity receptor. Surprisingly, and in spite of the severe reduction of TCR-induced IL-2 cytokine production, CD3/CD28 ligation–induced expression of CD25 (as well as the activation markers CD69 and CD44) was not significantly reduced in PKCθ$^{\Delta/\Delta}$ T cells when compared with wild-type T cells (Fig. 4). This activation-induced CD25 expression in PKCθ$^{\Delta/\Delta}$ T cells was consistently observed, even when using a range of anti-CD3 concentrations (0.25–1 μg ml^{-1}, with or without 1 μg ml^{-1} anti-CD28) as well as stimulation time frames from 16 to 24 h (not depicted). Consistent with this almost normal expression of the high affinity IL-2R, the addition of exogenous IL-2 mostly rescued the proliferative defect in PKCθ$^{\Delta/\Delta}$ T cells (Fig. 2 A). A signal transducing pathway involving activation and translocation of other PKC isotype(s) and/or RasGRP family members may therefore regulate expression of CD25 (as well as CD69 and CD44). Alternatively, expression of CD25 in PKCθ$^{\Delta/\Delta}$ T cells might be rescued by the residual but still significant IL-2 production of these cells, known to activate CD25 expression independent of TCR signaling. CD25 transcription is now known to be controlled by binding of HMG-I(Y), Stat5a, and Stat5b in vivo to upstream positive regulatory regions III and IV, which function as IL-2 response elements (25). Of note, similar reduction of IL-2 cytokine production but almost normal CD25 expression has been described in itk-deficient T cells (26).

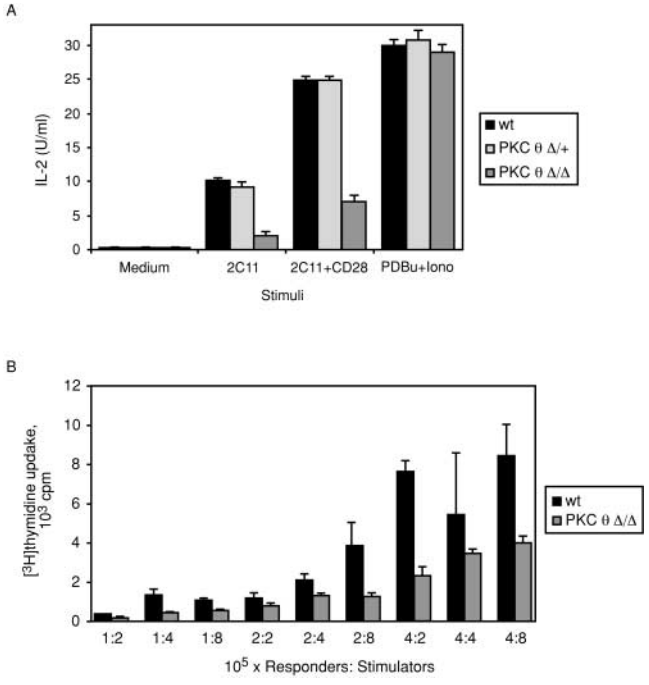

Figure 3. Impaired IL-2 secretion in PKCθ$^{\Delta/\Delta}$ mice. IL-2 cytokine secretion responses of (A) purified mature CD3$^+$ T cells of wild-type$^{+/+}$, PKCθ$^{\Delta/+}$, and PKCθ$^{\Delta/\Delta}$. IL-2 concentration in the supernatants of culture treated with various stimuli: medium, anti-CD3 (precoated with a concentration of 10 μg ml^{-1}), 1 μg ml^{-1} soluble anti-CD28, 10 ng ml^{-1} PDBu, and 1 μg ml^{-1} ionomycin, as indicated. IL-2 produced from the cultures was measured by quantifying the proliferation of the IL-2–dependent indicator cell line CTLL-2. Cells were then harvested and analyzed using standard procedures. (B) For the mixed lymphocyte reaction assays, purified mature CD3$^+$ T cells of wild-type$^{+/+}$ and PKCθ$^{\Delta/\Delta}$ littermates were mixed in duplicates at various densities with mitomycin C–treated splenocytes from BALB/c mice, as indicated. After 48 h of growth, the cells were pulsed for 16 h with 1 μCi [^{3}H]thymidine. Results shown are the mean ± SD [^{3}H]thymidine incorporation of at least four independent experiments.

PKCθ Is Essential for Antigen Receptor–induced NFAT Activation. To further elucidate the molecular basis of the impairment in antigen receptor signaling in the absence of PKCθ, we analyzed the critical NF-κB, AP-1, and NFAT pathways, known to be PKC dependent (27) and critical in TCR/CD28-induced IL-2 cytokine expression (28–31). Electrophoretic mobility shift assays (EMSAs) demonstrated that substantial NF-κB, AP-1, and NFAT DNA binding activity was induced in wild-type CD3$^+$ mature T cells after anti-CD3/anti-CD28 stimulation. In contrast, a significant albeit partial decrease in NF-κB and AP-1 activation in PKCθ$^{\Delta/\Delta}$ cells has been reproducibly observed (Fig. 5, A and B). Most surprisingly, CD3 cross-linking completely failed to fully activate the calcineurin-dependent transcription factors NFATp (=NFAT1) and NFATc (=NFAT2) in these cells (Fig. 5 C). Establishing a time course of CD3/CD28-induced NFAT activation, a significant decrease in NFAT DNA binding in PKCθ$^{\Delta/\Delta}$ cells has been reproducibly observed at 4, 8, and particularly at 16 h (Fig. 5 D), consistent with the observed lack of full T cell activation in PKCθ$^{\Delta/\Delta}$ T cells.

To exclude protein expression defects of the transcription factors studied, total cell extracts of resting and stimulated T cells from both wild-type and PKCθ$^{\Delta/\Delta}$ T cells were investigated. As a result, the activation-dependent up-regulation of fos, jun (Fig. 6 A), and the induction of the three prominent isoforms of NFATc (32) as well as NFATp was not altered in the PKCθ$^{\Delta/\Delta}$ T cells (Fig. 6, B and C), excluding signaling defects caused by simply different expression levels. However, the expression of p50$^{\text{NF-κB}}$ was significantly reduced in PKCθ-deficient T cells (Fig. 6

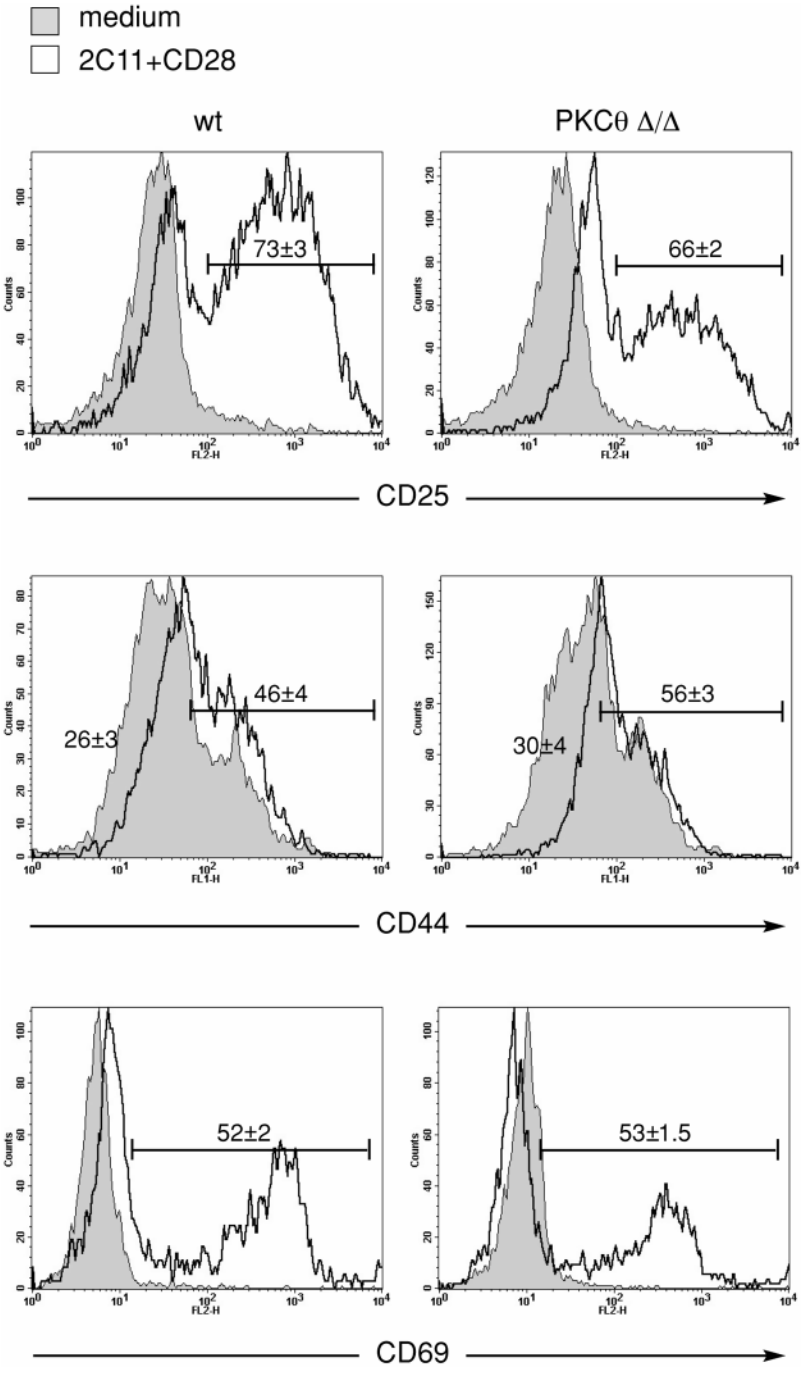

Figure 4. Flow cytometric analysis of expression of CD25, CD44, and CD69 on PKCθ$^{\Delta/\Delta}$ T cells. Single cell suspensions of purified mature CD3$^+$ T cells stimulated or not for 16 h with anti-CD3 and anti-CD28, were stained with anti-CD25, anti-CD44, and anti-CD69. Percentages of positive cells are indicated. Experiments were repeated at least three times in duplicates with similar results.

A), potentially indicating such an indirect effect in the NF-κB signaling pathway of PKCθ$^{\Delta/\Delta}$ T cells.

PKCθ Is Required for the Antigen Receptor–induced Calcium Signal. Given the greatly reduced TCR-induced NFAT activation in our PKCθ$^{\Delta/\Delta}$-derived T lymphocytes, we investigated if PKCθ might regulate TCR-induced Ca^{2+} mobilization, and subsequently downstream calcineurin and NFAT transactivation. We loaded mature CD3$^+$ T cells taken from PKCθ$^{\Delta/\Delta}$ and wild-type T cells with the intracellular Ca^{2+} indicator dye fura-2 and imaged increase of intracellular Ca^{2+} over time in response to the cross-linking of biotinylated anti-CD3 antibodies by streptavidin. Unexpectedly, we were able to distinguish different patterns of intracellular Ca^{2+} elevation and PKCθ$^{\Delta/\Delta}$ T cells failed to mobilize similar intracellular Ca^{2+} levels compared with wild-type littermates (Fig. 7 A). Wild-type T cells reproducibly demonstrate a steeper onset of Ca^{2+} signal (Fig. 7 B) with total cytosolic Ca^{2+} levels remaining roughly 60–80 nM higher than in the PKCθ$^{\Delta/\Delta}$ T cells (Fig. 7 C). Ca^{2+} responses in cells stimulated by Ca^{2+} ionophore remained intact in PKCθ-deficient T cells (Fig. 7 A). This might be explained by ionomycin's ability to deplete internal stores of

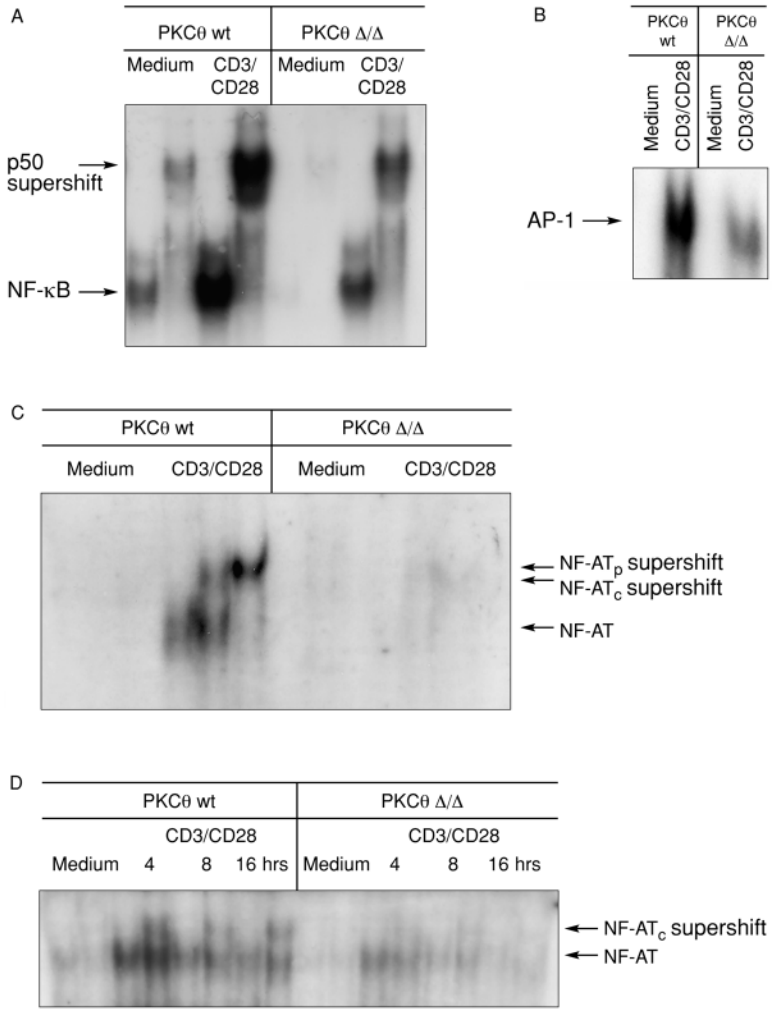

Figure 5. EMSA analysis of NF-κB, AP-1, and NFAT in PKCθ$^{\Delta/\Delta}$ T cells. Nuclear extracts were prepared from purified mature CD3$^+$ wild-type and PKCθ$^{\Delta/\Delta}$ T cells stimulated for 16 h with medium alone or plate-bound anti-CD3 plus soluble anti-CD28 as indicated. Gel mobility shift assays were performed using radiolabeled probes containing either (A) NF-κB, (B) AP-1, and (C and D) NFAT-binding site sequences. (D) To study the time course of NFAT activation, CD3$^+$ T cells were stimulated for 4, 8, and 16 h with anti-CD3 plus anti-CD28 or medium alone as indicated. The specificity of p50 NF-κB as well as NFATc and NFATp was confirmed by supershifting the electrophoretic mobility shift with antibodies as indicated by the arrow. Experiments were repeated at least three times with similar results.

Ca^{2+} as well as its direct effect on the plasma membrane. Given the identical CD3 surface expression in both T cell populations (Table I and not depicted), the stronger, i.e., more rapid response in wild-type T cells might indicate a different sensitivity state, with only this robust wild-type Ca^{2+} response correlating with sustained NFAT transactivation (refer to Fig. 5 D).

Ca^{2+} mobilization in T cells is initiated by membrane association and enzymatic activation of PLCγ1, which catalyzes the breakdown of phosphatidylinositol-4, 5-bisphosphate into IP_3, a stimulant for Ca^{2+} store depletion. Wild-type cells showed maximal IP_3 levels within 30 s after stimulation, consistent with rapid activation of PLCγ1 (Fig. 7 D). In contrast, the TCR-driven production of IP_3 was significantly albeit partially diminished in PKCθ$^{\Delta/\Delta}$ T cells, indicating that this partial defect might be the cause of altered Ca^{2+} mobilization in these cells. In addition, anti-CD3 stimulation revealed no apparent differences in the phosphorylation of Erk1/Erk2 (Fig. 7 E) in PKCθ$^{\Delta/\Delta}$ T cells. Of note, CD3-induced tyrosine phosphorylation at Y^{783} of PLCγ1 was not significantly changed in PKCθ$^{\Delta/\Delta}$ T cells (not depicted), consistent with the moderate reduction of PLCγ1 activation in these cells.

These data suggest that PKCθ physiologically operates upstream of the membrane-associated Ca^{2+} signaling scaffold in T cells, which mainly comprises the transmembrane adaptor protein LAT, the cytosolic adaptor proteins Gads and SLP-76, and the effector molecules PLCγ1 and itk (a PTK of the Tec family). Along this line of argumentation, in T cell lines we have shown that PKCθ (but not PKCα) membrane recruitment is, at least in part, independent of PLCγ1 (19). Second, and again consistent with this hypothesis, a very rapid and complete cytosol to membrane translocation of endogenous PKCθ, and to a lesser degree of endogenous PKCα, could be observed already after 1 min of CD3 cross-linking (Fig. 7 F).

Discussion

Proliferation of T cells after cross-linking of the TCR is a consequence of up-regulated transcription of the IL-2 cytokine gene. IL-2 expression requires NFAT activation, synthesis, phosphorylation, and activation of members of the Fos and Jun families as well as activity of NF-κB. All critical transcription factors act synergistically on composite DNA elements within the IL-2 promoter (27–29, 33, 34).

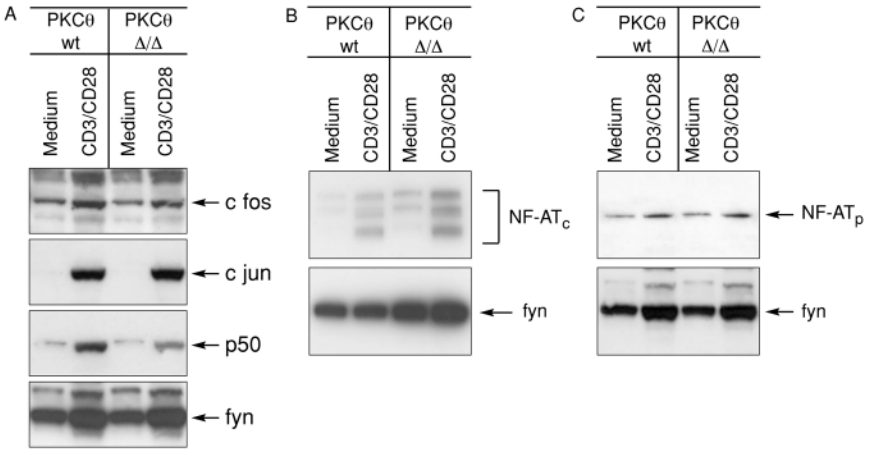

Figure 6. Protein expression analysis of p50, cfos, cjun, and NFAT in PKCθ$^{\Delta/\Delta}$ T cells. To control for the normal levels of protein expression of the transcription factors studied in EMSA, whole cell extracts of resting and 16 h–activated T cells were immunostained with the specific antibodies as indicated. Immunostaining of p59^{fyn} served as equal protein loading control.

As shown in this study, PKCθ$^{\Delta/\Delta}$ T cells failed to proliferate in response to TCR stimulation (Fig. 2 A) or allogenic MHC (Fig. 3 B). The reduced proliferative response was due to markedly decreased levels of IL-2 (Fig. 3 A). Consistently, in PKCθ$^{\Delta/\Delta}$ T cells, TCR/CD28-induced NF-κB and AP-1 activation was significantly reduced and NFAT activation was abrogated below the detection level (Figs. 5 and 6). The distal NFAT site within the IL-2 promoter is

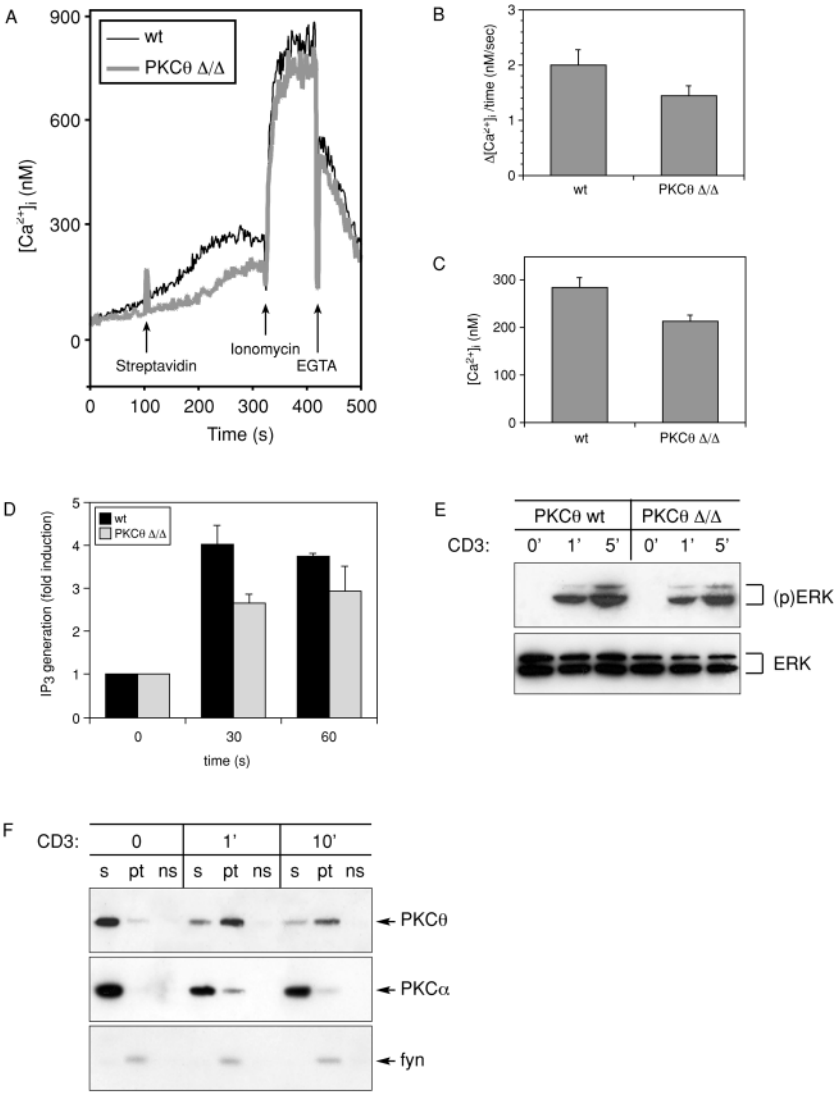

Figure 7. PKCθ is required for normal TCR-driven calcium mobilization but not for ERK activation. (A) Purified mature CD3$^+$ T cells (purified from pooled spleen and lymph nodes) were loaded with Fura-2 and monitored for changes in intracellular-free calcium $[Ca^{2+}]_i$. CD3 cross-linking was induced by streptavidin and direct Ca^{2+} influx with ionomycin. (B and C) Ca^{2+} signaling patterns from four representative experiments performed in duplicates are statistically analyzed. Slope (B, nM/s) and plateau (C, nM) of intracellular Ca^{2+} varied significantly in PKCθ-deficient cells ($P < 0.01$). (D) Graphs showing the mean levels of IP_3 stimulated by cross-linking of CD3 as above for 0, 30, and 60 s. Detected IP_3 levels ranged from 0.2 pmol/10^7 cells (unstimulated cells) to 0.8 pmol/10^7 cells (wild-type stimulated cells). Results shown are the mean ± SD of at least three independent experiments. (E) Total cell lysates were immunostained sequentially with anti–phospho-MAPK that detects dually phosphorylated (active) ERK1, ERK2, and anti-ERK1/2 that recognizes pan-ERK. (F) Kinetics of subcellular translocation of endogenous PKC isotypes in Jurkat T cells as indicated. The cell fractions are defined as the soluble (s, cytosol) fraction, the particulate (pt, predominantly plasma membrane) fraction, and the NP-40 nonsoluble fraction (ns, predominantly cytoskeleton, detergents insoluble membrane domains). As internal control for cell fractionation, immunostaining of p59^{fyn} predominantly recognized the particulate fraction.

known to cooperatively bind NFAT and AP-1 (35), and therefore the relative contribution of PKCθ to NFAT versus AP-1 activation is not yet resolved. Nevertheless, TCR-induced sustained Ca^{2+} mobilization was altered and significantly reduced in PKCθ$^{\Delta/\Delta}$ T cells (Fig. 7 A), indicating that the Ca^{2+}/NFAT pathway might play a critical role in the IL-2 promoter activation by PKCθ. Of note, the reduced Ca^{2+} mobilization in PKCθ$^{\Delta/\Delta}$ T cells might potentially explain, at least in part, the observed partial reduction of NF-κB and AP-1 transactivation, signaling pathways both known to be sensitive to the amplitude and duration of the Ca^{2+} signal (6, 36).

Sun et al. (14) partially inactivated the PKCθ gene by homologous recombination by replacing the exon 11 (with a neomycin resistance gene expression cassette). These two distinct PKCθ knockout mouse lines (14 and this study) are identical in regard to their genetic background (129-C57BL/6J). Consistent with the phenotype of our null allele PKCθ$^{\Delta/\Delta}$, T cell development was shown to be unaffected in the absence of PKCθ and PKCθ$^{\Delta/\Delta}$ T cells did produce less IL-2 and failed to proliferate strongly in response to TCR stimulation (14). Surprisingly, however, major discrepancies have been observed (Table II). Mature T lymphocytes from PKCθ heterozygous mice show normal TCR-induced IL-2 responses (haplosufficiency, Fig. 3 A) but impaired IL-2 responses (haploinsufficiency) in the studies of Sun et al. (14). In addition, PKCθ$^{\Delta/\Delta}$ T cells did produce normal PDBu and ionomycin induced proliferation (Fig. 2 B) and IL-2 secretion (Fig. 3 A) as well as normal CD3/CD28-induced up-regulation of CD25 (as well as CD69) surface expression (Fig. 4). These signal pathways, however, were shown to be impaired by Sun et al. (14). Next and most importantly, the PKCθ$^{\Delta/\Delta}$-derived mature T cells in our current study are primarily defective in TCR-mediated NFAT signaling (Fig. 5), but Sun et al. (14) observed completely normal TCR-induced NFAT activation in their PKCθ T cells. Thus, studies of these two different PKCθ knockouts reveal certain fundamental differences. Differences might be explained by unintended defects from a particular targeting strategy, which may include dominant-negative effects of expressed anomalous protein or alterations in nearby genes. Such differences warrant further investigation.

Activation of T lymphocytes through the TCR includes IP_3-mediated elevation of cytosolic $[Ca^{2+}]_i$ initiated by Ca^{2+} release from internal stores and subsequent capacitative Ca^{2+} entry (CCE) through stores-operated Ca^{2+} channels. CCE is an absolute requirement for normal T cell activation, i.e., the elevation of $[Ca^{2+}]_i$ must be sustained for commitment of the lymphocyte to maintain NFAT transcription factors in the nucleus (37) to induce transcription of the cytokine IL-2 (31). Consistent with our observed NFAT defect, TCR-induced sustained Ca^{2+} mobilization was altered and significantly albeit partially reduced in

Table II. *Comparison of Two Independent PKCθ Knockout Strains*

	Sun et al. (reference 14)	This study
Targeting strategy:	Exon 11 replaced by PKG-neo	Cre/loxP null allele (deletion of exons 3 and 4)
Residual open reading frame	365 aa	9 aa
Thymocytes:		
Development	normal	normal
Peripheral T cells:		
Proliferative responses		
to CD3/CD28	impaired	impaired
to PMA/ionomycin	impaired	**normal**
to allogenic MHC	partially impaired	partially impaired
IL-2 production		
to CD3/CD28	impaired	impaired
to PMA/ionomycin	impaired	**normal**
Heterozygous phenotype:	impaired	**normal**
EMSA/stimulated with CD3/CD28		
NF-κB	impaired	**partially impaired**
AP-1	impaired	**partially impaired**
NFAT	normal	**impaired**
Surface expression/stimulated with CD3/CD28		
CD69	impaired	**normal**
CD25	impaired	**normal**

PKCθ$^{\Delta/\Delta}$ T cells (Fig. 7 A). This may very well indicate subcellular signaling defects that can limit the intensity and duration of highly localized Ca^{2+} spikes. The Ca^{2+} mobilization defect in the PKCθ-deficient T cells might be due to any defect in membrane association and enzymatic activation of PLCγ1, which catalyzes the breakdown of phosphatidylinositol-4, 5-bisphosphate into IP_3, a stimulant for Ca^{2+} mobilization (for review see 38). Indeed, upon CD3 cross-linking, the overall IP_3 production in the PKCθ$^{\Delta/\Delta}$ T cell was found to be partially reduced (Fig. 7 D), suggesting that PLCγ1 is less efficiently stimulated in PKCθ-deficient T cells. Nevertheless, additional downstream defects of release of Ca^{2+} stores, disruption of the signal between Ca^{2+} stores release and Ca^{2+} entry, and direct block of the Ca^{2+} entry channels that produce CCE in PKCθ-deficient T cells cannot be excluded at this point.

Current models suggest that immune responses in T lymphocytes are exquisitely controlled, requiring multiple finely tuned levels of activation signals. Even a small disturbance of the full Ca^{2+} signal may therefore correlate with an inability of the stimulus to induce stimulation of calcineurin, which leads to dephosphorylation and nuclear localization of NFAT (31, 37). Similarly, it has been shown that a sustained elevation of the intracellular Ca^{2+} concentration is necessary for the activation of the IL-2 promoter (39). If $[Ca^{2+}]_i$ declines too early after TCR stimulation, a reverse translocation of NFAT out of the nucleus will occur (37, 40), thus aborting the immune response. From the data of Karttunen and Shastri (41) and Valitutti et al. (42), it also appears that a full and sustained Ca^{2+} stimulus must be maintained to induce an irreversible commitment to T cell activation, particularly at lower antigenic peptide concentrations. Consistently, immunomodulatory drugs (cyclosporin A, FK506) are used that target calcineurin and inhibit translocation of NFAT. Clinical studies demonstrate that the dose of cyclosporin A necessary to prevent transplant rejection inhibits only ~50% of calcineurin activity in lymphocytes but is sufficient to abrogate nuclear localization of NFATc family members (for review see 33). Along this line of argumentation, PKCθ-deficient T cells generate still detectable, albeit significantly reduced, Ca^{2+} responses. Given the importance of the sustained phase of the Ca^{2+} signal, such a small reduction of intracellular Ca^{2+} ion concentration might correlate with an inability of the stimulus to induce IL-2 gene expression and T cell proliferation. Thus, PKCθ, unlike the more proximally acting Lck and ZAP70, may not serve as primary trigger of the immune response but instead may further refine lymphocyte signaling by acting as a critical signal strength regulator of PLCγ1 activation, i.e., as a rate-limiting step in triggering a full T cell Ca^{2+} signal during antigenic stimulation. Similarly, such a partial suppression of PLCγ1 has been described, i.e., in the itk-deficient T cells (26).

Taken together, this suggests that PKCθ is part of a signaling pathway that is necessary for full T cell activation and the observed reduction in the IP_3 production and subsequent Ca^{2+} response might be responsible for the observed primary defect of NFAT transactivation in PKCθ$^{\Delta/\Delta}$ T cells. Thus, PKCθ appears critical for efficient signaling downstream of the TCR and the primary effect of PKCθ loss of function may lie upstream of TCR-induced Ca^{2+} mobilization. How the loss of PKCθ results in defective Ca^{2+} responses needs to be investigated.

We are grateful to Drs. H. Dietrich, N. Hermann, N. Krumböck, and G. Böck (all from Innsbruck) for animal house keeping and expert technical assistance including FACS® analysis. All experiments comply with the current laws of Austria.

This work was supported by a grant of the Austrian Science Fund (P14394-BIO and P16229-B07) and by a cooperation agreement with Altana Pharma (Konstanz, Germany).

Submitted: 11 February 2002
Revised: 27 November 2002
Accepted: 8 April 2003

References

1. Baier, G. 2003. The PKC gene module: molecular biosystematics to resolve its T cell functions. *Immunol. Rev.* 192: 64–79.
2. Baier, G., D. Telford, L. Giampa, K.M. Coggeshall, G. Baier-Bitterlich, N. Isakov, and A. Altman. 1993. Molecular cloning and characterization of PKCθ, a novel member of the protein kinase C (PKC) gene family expressed predominantly in hematopoietic cells. *J. Biol. Chem.* 268:4997–5004.
3. Baier, G., G. Baier-Bitterlich, N. Meller, K.M. Coggeshall, L. Giampa, D. Telford, N. Isakov, and A. Altman. 1994. Expression and biochemical characterization of human PKCθ. *Eur. J. Biochem.* 225:195–203.
4. Wilda, M., N. Ghaffari-Tabrizi, I. Reisert, G. Utermann, G. Baier, and H. Hameister. 2001. Protein kinase C isoenzyme: selective expression pattern of PKCθ; during mouse development. *Mech. Dev.* 103:197–200.
5. Baier-Bitterlich, G., F. Uberall, B. Bauer, F. Fresser, H. Wachter, H. Grunicke, G. Utermann, A. Altman, and G. Baier. 1996. PKCθ isoenzyme selective stimulation of the transcription factor complex AP-1 in T lymphocytes. *Mol. Cell. Biol.* 16:1842–1850.
6. Werlen, G., E. Jacinto, Y. Xia, and M. Karin. 1998. Calcineurin preferentially synergizes with PKCθ to activate JNK and IL2 promoter in T lymphocytes. *EMBO J.* 17:3101–3111.
7. Ghaffari-Tabrizi, N., B. Bauer, A. Villunger, G. Baier-Bitterlich, A. Altman, G. Utermann, F. Uberall, and G. Baier. 1999. PKCθ, a selective upstream regulator of JNK/SAPK and IL2 promoter activation in Jurkat T cells. *Eur. J. Immunol.* 29:132–142.
8. Bauer, B., N. Krumbock, N. Ghaffari-Tabrizi, S. Kampfer, A. Villunger, M. Wilda, H. Hameister, G. Utermann, M. Leitges, F. Uberall, et al. 2000. T cell expressed PKCθ demonstrates cell-type selective function. *Eur. J. Immunol.* 30: 3645–3654.
9. Lin, X., A. O'Mahony, Y. Mu, R. Geleziunas, and W.C. Greene. 2000. PKCθ participates in NF-κB activation induced by CD3-CD28 costimulation through selective activation of IκB kinase β. *Mol. Cell. Biol.* 20:2933–2940.
10. Coudronniere, N., M. Villalba, N. Englund, and A. Altman. 2000. NF-κB activation induced by T cell receptor/CD28 costimulation is mediated by PKCθ. *Proc. Natl. Acad. Sci. USA.* 97:3394–3399.

11. Khoshnan, A., D. Bae, C.A. Tindell, and A.E. Nel. 2000. The physical association of PKCθ with a lipid raft-associated inhibitor of κ B factor kinase (IKK) complex plays a role in the activation of the NF-κB cascade by TCR and CD28. *J. Immunol.* 165:6933–6940.
12. Kane, L.P., P.G. Andres, K.C. Howland, A.K. Abbas, and A. Weiss. 2001. Akt provides the CD28 costimulatory signal for up-regulation of IL-2 and INFγ but not Th2 cytokines. *Nat. Immunol.* 2:37-44.
13. Bauer, B., N. Krumbock, F. Fresser, F. Hochholdinger, M. Spitaler, A. Simm, F. Uberall, B. Schraven, and G. Baier. 2001. Complex formation and cooperation of PKCθ and Akt1/PKB-α in the NF-κB transactivation cascade in Jurkat T cells. *J. Biol. Chem.* 276:31627–31634.
14. Sun, Z., C.W. Arendt, W. Ellmeier, E.M. Schaeffer, M.J. Sunshine, L. Gandhi, J. Annes, D. Petrzilka, A. Kupfer, P.L. Schwartzberg, et al. 2000. PKCθ is required for TCR-induced NF-κB activation in mature but not immature T lymphocytes. *Nature.* 404:402–407.
15. Monks, C.R., H. Kupfer, I. Tamir, A. Barlow, and A. Kupfer. 1997. Selective modulation of PKCθ during T-cell activation. *Nature.* 385:83–86.
16. Huang, J., P.F. Lo, T. Zal, N.R. Gascoigne, B.A. Smith, S.D. Levin, and H.M. Grey. 2002. CD28 plays a critical role in the segregation of PKCθ within the immunologic synapse. *Proc. Natl. Acad. Sci. USA.* 99:9369–9373.
17. Kong, Y.Y., K.D. Fischer, M.F. Bachmann, S. Mariathasan, I. Kozieradzki, M.P. Nghiem, D. Bouchard, A. Bernstein, P.S. Ohashi, and J.M. Penninger. 1998. Vav regulates peptide-specific apoptosis in thymocytes. *J. Exp. Med.* 188:2099–2111.
18. Villalba, M., N. Coudronniere, M. Deckert, E. Teixeiro, P. Mas, and A. Altman. 2000. A novel functional interaction between Vav and PKCθ is required for TCR-induced T cell activation. *Immunity.* 12:151–160.
19. Villalba, M., K. Bi, J. Hu, Y. Altman, P. Bushway, E. Reits, J. Neefjes, G. Baier, R.T. Abraham, and A. Altman. 2002. Translocation of PKCθ in T cells is mediated by a nonconventional, PI3-K– and Vav-dependent pathway, but does not absolutely require phospholipase C. *J. Cell Biol.* 157:253–263.
20. Nishizuka, Y. 1992. Intracellular signaling by hydrolysis of phospholipids and activation of protein kinase C. *Science.* 258:607–614.
21. Kofler, K., S. Kochl, W. Parson, M. Erdel, G. Utermann, and G. Baier. 1998. Molecular characterization of the human PKCθ gene locus (PRKCQ). *Mol. Gen. Genet.* 259:398–403.
22. Oberhuber, H., K. Maly, F. Uberall, J. Hoflacher, A. Kiani, and H.H. Grunicke. 1991. Mechanism of desensitization of the Ca2+ mobilizing system to bombesin by Ha-ras. Independence from down-modulation of agonist-stimulated inositol phosphate production. *J. Biol. Chem.* 266:1437–1442.
23. Grynkiewicz, G., M. Poenie, and R.Y. Tsien. 1985. A new generation of Ca2+ indicators with greatly improved fluorescence properties. *J. Biol. Chem.* 260:3440–3450.
24. Niino, Y.S., T. Irie, M. Takaishi, T. Hosono, N. Huh, T. Tachikawa, and T. Kuroki. 2001. PKCθII, a new isoform of protein kinase C specifically expressed in the seminiferous tubules of mouse testis. *J. Biol. Chem.* 276:36711–36717.
25. Kim, H.P., and W.J. Leonard. 2002. The basis for TCR-mediated regulation of the IL-2 receptor α chain gene: role of widely separated regulatory elements. *EMBO J.* 21:3051–3059.
26. Schaeffer, E.M., J. Debnath, G. Yap, D. McVicar, X.C. Liao, D.R. Littman, A. Sher, H.E. Varmus, M.J. Lenardo, and P.L. Schwartzberg. 1999. Requirement for Tec kinases Rlk and Itk in T cell receptor signaling and immunity. *Science.* 284: 638–641.
27. Altman, A., N. Isakov, and G. Baier. 2000. PKCθ: a new essential superstar on the T-cell stage. *Immunol. Today.* 21:567–573.
28. Weiss, A., and D.R. Littman. 1994. Signal transduction by lymphocyte antigen receptors. *Cell.* 76:263–274.
29. Rothenberg, E.V., and S.B. Ward. 1996. A dynamic assembly of diverse transcription factors integrates activation and cell-type information for IL-2 gene regulation. *Proc. Natl. Acad. Sci. USA.* 93:9358–9365.
30. Jain, J., C. Loh, and A. Rao. 1995. Transcriptional regulation of the IL-2 gene. *Curr. Opin. Immunol.* 7:333–342.
31. Crabtree, G.R. 1999. Generic signals and specific outcomes: signaling through Ca2+, calcineurin, and NF-AT. *Cell.* 96: 611–614.
32. Chuvpilo, S., M. Zimmer, A. Kerstan, J. Glockner, A. Avots, C. Escher, C. Fischer, I. Inashkina, E. Jankevics, F. Berberich-Siebelt, et al. 1999. Alternative polyadenylation events contribute to the induction of NF-ATc in effector T cells. *Immunity.* 10:261–269.
33. Neilson, J., K. Stankunas, and G.R. Crabtree. 2001. Monitoring the duration of antigen-receptor occupancy by calcineurin/glycogen-synthase-kinase-3 control of NF-AT nuclear shuttling. *Curr. Opin. Immunol.* 13:346–350.
34. Macian, F., C. Lopez-Rodriguez, and A. Rao. 2001. Partners in transcription: NF-AT and AP-1. *Oncogene.* 20:2476–2489.
35. Macian, F., C. Garcia-Rodriguez, and A. Rao. 2000. Gene expression elicited by NF-AT in the presence or absence of cooperative recruitment of Fos and Jun. *EMBO J.* 19:4783–4795.
36. Trushin, S.A., K.N. Pennington, A. Algeciras-Schimnich, and C.V. Paya. 1999. Protein kinase C and calcineurin synergize to activate IκB kinase and NF-κB in T lymphocytes. *J. Biol. Chem.* 274:22923–22931.
37. Timmerman, L.A., N.A. Clipstone, S.N. Ho, J.P. Northrop, and G.R. Crabtree. 1996. Rapid shuttling of NF-AT in discrimination of Ca2+ signals and immunosuppression. *Nature.* 383:837–840.
38. Leo, A., J. Wienands, G. Baier, V. Horejsi, and B. Schraven. 2002. Adapters in lymphocyte signaling. *J. Clin. Invest.* 109: 301–309.
39. Negulescu, P.A., N. Shastri, and M.D. Cahalan. 1994. Intracellular calcium dependence of gene expression in single T lymphocytes. *Proc. Natl. Acad. Sci. USA.* 91:2873–2877.
40. Shibasaki, F., E.R. Price, D. Milan, and F. McKeon. 1996. Role of kinases and the phosphatase calcineurin in the nuclear shuttling of transcription factor NF-AT4. *Nature.* 382: 370–373.
41. Karttunen, J., and N. Shastri. 1991. Measurement of ligand-induced activation in single viable T cells using the lacZ reporter gene. *Proc. Natl. Acad. Sci. USA.* 88:3972–3976.
42. Valitutti, S., M. Dessing, K. Aktories, H. Gallati, and A. Lanzavecchia. 1995. Sustained signaling leading to T cell activation results from prolonged T cell receptor occupancy. Role of T cell actin cytoskeleton. *J. Exp. Med.* 181:577–584.